Symmetry breaking and manipulation of nonlinear optical modes in an asymmetric double-channel waveguide

Rujiang Li,[1] Fei Lv,[1] Lu Li,[1,*] and Zhiyong Xu[2]

[1]*Institute of Theoretical Physics, Shanxi University, Taiyuan 030006, China*

[2]*Nonlinear Physics Centre, Research School of Physics and Engineering, Australian National University, Canberra, Australian Capital Territory 0200, Australia*

(Received 8 June 2011; published 28 September 2011)

We study light-beam propagation in a nonlinear coupler with an asymmetric double-channel waveguide and derive various analytical forms of optical modes. The results show that the symmetry-preserving modes in a symmetric double-channel waveguide are deformed due to the asymmetry of the two-channel waveguide, yet such a coupler supports the symmetry-breaking modes. The dispersion relations reveal that the system with self-focusing nonlinear response supports the degenerate modes, while for self-defocusing medium the degenerate modes do not exist. Furthermore, nonlinear manipulation is investigated by launching optical modes supported in double-channel waveguide into a nonlinear uniform medium.

DOI: 10.1103/PhysRevA.84.033850 PACS number(s): 42.65.Tg, 42.65.Jx, 42.65.Wi

I. INTRODUCTION

Propagation of optical waves in waveguide arrays has become an important and effective means to investigate various optical phenomena which have analogs in many fields of physics [1]. Special attention has been paid to nonlinear surface waves and nonlinear guided waves in planar layered structures [2–13] and nonlinear couplers [14–18], generation and properties of solitons in nonlinear waveguide arrays [19–24], and other nonlinear periodic systems, such as optically induced lattices [25–28]. Light-beam propagation in waveguide arrays attracts attention because of the potential applications in all-optical signal processing in fiber optic networks and devices, passive mode locking using waveguide arrays [29], and beam steering [30–32].

The behavior of light-beam propagation in a coupler composed of a two-channel nonlinear waveguide gained particular attention because it can exhibit some universal properties in nonlinear periodic systems and nonlinear waveguide arrays [33]. The coupler can support symmetry-preserving solutions, which have linear counterparts, and symmetry-breaking solutions without any linear counterparts [34–36], in which the spontaneous symmetry breaking has been experimentally demonstrated in optically induced lattices with a local double-well potential [34].

In this paper, we consider light-beam propagation in an asymmetric double-channel waveguide with Kerr-type nonlinear response and derive various analytical stationary solutions in detail. It is found that the asymmetric double-channel waveguide can break the symmetric form of the symmetry-preserving modes in the otherwise symmetric double-channel waveguide, and such a coupler supports the symmetry-breaking modes. We also investigate how the type of nonlinear response affects the existence and properties of nonlinear optical modes in the asymmetric double-channel waveguide. The dispersion relation shows that the degenerate modes exist in the system with self-focusing nonlinear response, while for the coupler with self-defocusing response, the degenerate modes do not exist. In addition, based on these optical modes supported in asymmetric double-channel waveguide, we demonstrate the control and manipulation of optical modes in different nonlinear media by tuning the waveguide parameters.

The paper is organized as follows. In Sec. II, the model equation describing beam propagation in a double-channel waveguide is derived. In Sec. III, various analytical forms of optical modes are presented both in self-focusing and self-defocusing media. Meanwhile, the dispersion relations between the total energy and the propagation constant are discussed. In Sec. IV, we study the nonlinear manipulation of optical modes in a double-channel waveguide. Our findings are summarized in Sec. V.

II. MODEL EQUATION AND REDUCTIONS

We consider a planar graded-index waveguide with refractive index

$$n(z,x) = F(x) + n_2 I(z,x). \tag{1}$$

Here, the first term on the right-hand side presents a two-channel waveguide with the different refractive index, namely, $F(x) = n_{11}$ as $-L_0/2 - D_0 < x < -L_0/2$, $F(x) = n_{12}$ as $L_0/2 < x < L_0/2 + D_0$, and otherwise $F(x) = n_0$ ($< n_{11}, n_{12}$), where D_0 and L_0 represent the width of waveguide and the separation between waveguides, respectively. Variables n_0, n_{11}, and n_{12} denote the refractive index of cladding and waveguide, respectively. The second term denotes Kerr-type nonlinearity, $I(z,x)$ is the optical intensity, and positive (negative) values of nonlinear coefficient n_2 indicate self-focusing (self-defocusing) medium. Under slowly varying envelope approximation, the nonlinear wave equation governing beam propagation in such a waveguide with the refractive index given by Eq. (1) can be written as

$$i\frac{\partial\psi}{\partial z} + \frac{1}{2k_0}\frac{\partial^2\psi}{\partial x^2} + \frac{k_0[F(x) - n_0]}{n_0}\psi + \frac{k_0 n_2}{n_0}|\psi|^2\psi = 0, \tag{2}$$

*llz@sxu.edu.cn

where $\psi(z,x)$ is the envelope function and $k_0 = 2\pi n_0/\lambda$ is the wave number, with λ being the wavelength of the optical source generating the beam. By introducing the normalized transformations $\psi(z,x) = (k_0 |n_2| L_D/n_0)^{-1/2}\varphi(\zeta,\xi)$, $\xi = x/w_0$, and $\zeta = z/L_D$ with $L_D = 2k_0 w_0^2$, which represents the diffraction length, we get the dimensionless form of Eq. (2) as follows:

$$i\frac{\partial\varphi}{\partial\zeta} + \frac{\partial^2\varphi}{\partial\xi^2} + V(\xi)\varphi + \eta|\varphi|^2\varphi = 0, \tag{3}$$

where $\eta = n_2/|n_2| = \pm 1$ corresponds to self-focusing (+) and self-defocusing (−) nonlinearity of the waveguides, respectively, and $V(\xi) = 2k_0^2 w_0^2 [F(w_0\xi) - n_0]/n_0$ is of the form

$$V(\xi) = \begin{cases} V_1, & -L/2 - D < \xi < -L/2, \\ V_2, & L/2 < \xi < L/2 + D, \\ 0, & \text{otherwise}, \end{cases} \tag{4}$$

which describes the dimensionless two-channel waveguide structure with different refractive indices, where $V_1 = 2k_0^2 w_0^2(n_{11} - n_0)/n_0$ and $V_2 = 2k_0^2 w_0^2(n_{12} - n_0)/n_0$ are the modulation depths of the refractive indices of the left and right waveguides and $L = L_0/w_0$ and $D = D_0/w_0$ correspond to scaled separation and width of the waveguides, respectively. Here, we use the typical waveguide parameters $D = 3.5$, $L = 5$, $V_2 = 2.525$, and vary V_1. Figure 1 shows the profile of the two-channel waveguide structure given by Eq. (4). It should be pointed out that such a structure can be realized experimentally [37]. Equation (3) conserves the total energy flow $P(\zeta) = \int_{-\infty}^{+\infty} |\varphi(\zeta,\xi)|^2 d\xi = P_0$, where P_0 is the dimensionless initial total energy.

Assuming that the stationary solution of Eq. (3) is of the form $\varphi(\zeta,\xi) = u(\xi)\exp(i\beta\zeta)$, where $u(\xi)$ is a real function and β is the propagation constant, by substituting it into Eq. (3) we find that the function $u(\xi)$ obeys the following nonlinear equation:

$$\frac{d^2u}{d\xi^2} + [V(\xi) - \beta]u + \eta u^3 = 0, \tag{5}$$

where $\eta = \pm 1$ corresponds to self-focusing (+) and self-defocusing (−) nonlinearity of the waveguides, respectively. It should be pointed out that Eq. (5) not only can describe the optical modes in the double-channel waveguide structure with the different refractive index but also can describe one-dimensional Bose-Einstein condensate trapped in a finite asymmetrical double-square-well potential $-V(\xi)$. In particular, when $V_1 = V_2$, the corresponding optical modes in the symmetric double-channel waveguide structure have been studied, and the results have shown that the coupler supports not only symmetry-preserving modes but also symmetry-breaking modes [36].

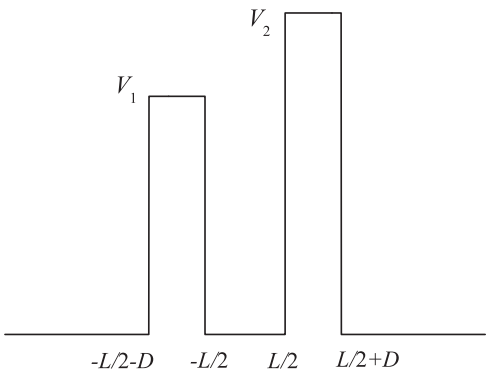

FIG. 1. The profile of a two-channel waveguide with different refractive indices.

III. OPTICAL MODES

In this section, we present the analytical solutions of Eq. (5) with the potential (4) for $\eta = \pm 1$. Generally, the solutions of Eq. (5) can be constructed in terms of the Jacobi elliptic functions depending on the values of the variable ξ and have the same propagation constants in different regions. Within the double-channel waveguides of $-L/2 - D < \xi < -L/2$ and $L/2 < \xi < L/2 + D$, the solution of Eq. (5) is the oscillatory function, so it can be selected in the form [38]

$$u_1(\xi; A, K, \delta) = A\,\mathrm{sn}\left(K\xi + \delta, -\frac{\eta A^2}{2K^2}\right), \tag{6}$$

with $\beta = V_1 - K^2 + \eta A^2/2$ in the region of $-L/2 - D < \xi < -L/2$ and $\beta = V_2 - K^2 + \eta A^2/2$ in the region of $L/2 < \xi < L/2 + D$. In the region of $|\xi| < L/2$, the solution of Eq. (5) has two different Jacobi elliptical functions for the symmetric and the antisymmetric case, respectively. For the symmetric case, the solution is [38]

$$u_2(\xi; B, Q, \sigma) = B\,\mathrm{nc}\left(Q\xi + \sigma, 1 + \frac{\eta B^2}{2Q^2}\right), \tag{7}$$

with $\beta = Q^2 + \eta B^2$; and for the antisymmetric case, the solution is [38]

$$u_2(\xi; B, Q, \sigma) = B\,\mathrm{sc}\left(Q\xi + \sigma, 1 + \frac{\eta B^2}{2Q^2}\right), \tag{8}$$

with $\beta = Q^2 - \eta B^2/2$. It should be noted that those two solutions are precise solutions of Eq. (5) for one node and no node within the region of $|\xi| < L/2$. In other regions, the solution of Eq. (5) is required to tend to zero as $\xi \to \pm\infty$, so it is taken as [36]

$$u_3(\xi; b) = \frac{1}{be^{-\sqrt{\beta}\xi} + ce^{\sqrt{\beta}\xi}}, \tag{9}$$

with $\beta > 0$. Substituting (9) into Eq. (5), one obtains $c = \eta/(8\beta b)$.

Note here that although the modulus in the usual Jacobi elliptic function is restricted from 0 to 1, this problem can be solved by the modular transformation such that the modulus in the Jacobi elliptic functions given by Eqs. (6) to (8) can take any positive or negative values in our investigations, as shown in Refs. [38,39], so those solutions do not depend on a nonlinearity sign.

In the following, we show the analytical global solutions of Eq. (5). With the help of Eqs. (6), (7) [or (8)], and (9), the

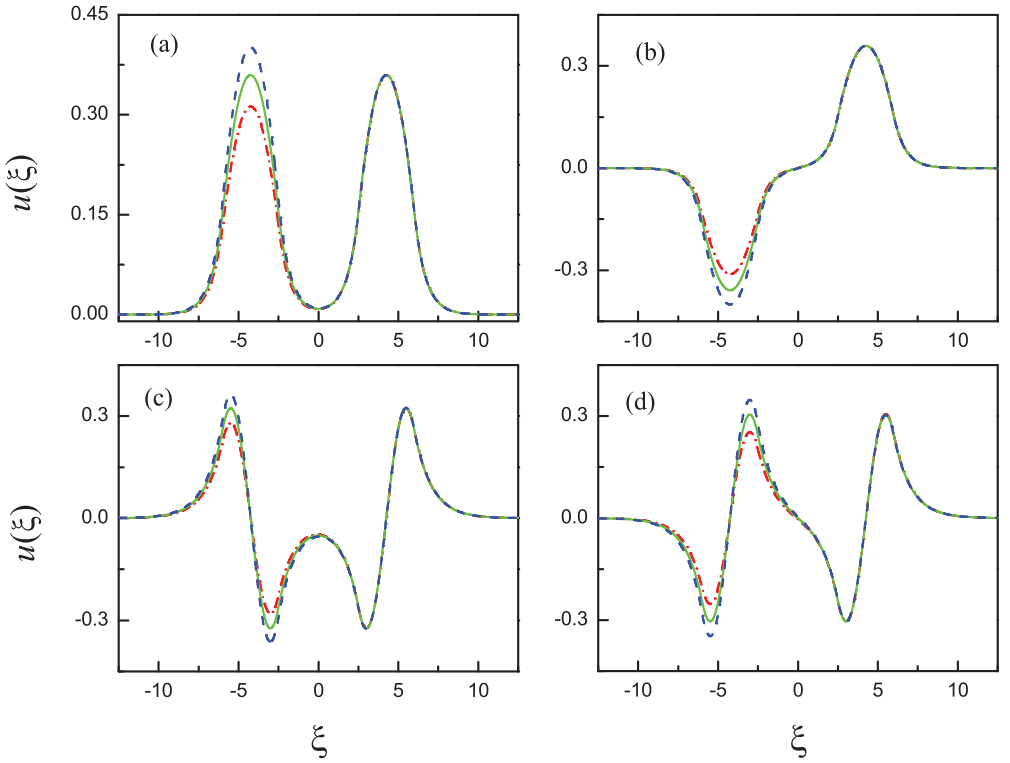

FIG. 2. (Color online) Various different optical modes existing in self-defocusing medium ($\eta = -1$), where the dash-dotted red line is the optical mode for $V_1 = 2.500$, the solid green line is the optical mode for $V_1 = 2.525$, and the dashed blue line is the optical mode for $V_1 = 2.550$. Here $\beta = 2.00$ in (a) and (b) and $\beta = 0.85$ in (c) and (d).

solutions of Eq. (5) can be written as

$$u(\xi) = \begin{cases} u_3(\xi; b_1), & \xi < -L/2 - D, \\ u_1(\xi; A_1, K_1, \delta_1), & -L/2 - D < \xi < -L/2, \\ u_2(\xi; B, Q, \sigma), & |\xi| < L/2, \\ u_1(\xi; A_2, K_2, \delta_2), & L/2 < \xi < L/2 + D, \\ u_3(\xi; b_2), & \xi > L/2 + D. \end{cases} \tag{10}$$

The continuity conditions for u and $\partial u/\partial\xi$ at the boundaries of $\xi = \pm L/2$ and $\xi = \pm(L/2 + D)$ require

$$\begin{aligned} u_3(-L/2 - D; b_1) &= u_1(-L/2 - D; A_1, K_1, \delta_1), \\ \frac{du_3}{d\xi}(-L/2 - D; b_1) &= \frac{du_1}{d\xi}(-L/2 - D; A_1, K_1, \delta_1), \\ u_1(-L/2; A_1, K_1, \delta_1) &= u_2(-L/2; B, Q, \sigma), \\ \frac{du_1}{d\xi}(-L/2; A_1, K_1, \delta_1) &= \frac{du_2}{d\xi}(-L/2; B, Q, \sigma), \\ u_2(L/2; B, Q, \sigma) &= u_1(L/2; A_2, K_2, \delta_2), \\ \frac{du_2}{d\xi}(L/2; B, Q, \sigma) &= \frac{du_1}{d\xi}(L/2; A_2, K_2, \delta_2), \\ u_1(L/2 + D; A_2, K_2, \delta_2) &= u_3(L/2 + D; b_2), \\ \frac{du_1}{d\xi}(L/2 + D; A_2, K_2, \delta_2) &= \frac{du_3}{d\xi}(L/2 + D; b_2), \end{aligned} \tag{11}$$

with $\beta = V_1 - K_1^2 + \eta A_1^2/2 = V_2 - K_2^2 + \eta A_2^2/2$ and $\beta = Q^2 + \eta B^2$ for the symmetric case given by Eq. (7) or $\beta = Q^2 - \eta B^2/2$ for the antisymmetric case given by Eq. (8). In Eq. (10), there are eleven parameters A_1, K_1, δ_1, A_2, K_2, δ_2, B, Q, σ, b_1, and b_2, which can be calculated by solving numerically Eqs. (11) with the conditions that the propagation constants in different regions should be same. Once those parameters are determined numerically, we can obtain the exact optical modes for asymmetric double-channel nonlinear waveguides.

Figures 2 and 3 show several different optical modes in a nonlinear asymmetric double-channel waveguide in the self-defocusing medium and the self-focusing medium, respectively. These optical modes are induced from the symmetry-preserving optical modes in the symmetric double-channel waveguide, where for comparison we also plotted the corresponding symmetry-preserving optical modes in the symmetric double-channel waveguides in the same figure. From Figs. 2 and 3, we found that the symmetry of the modes is broken due to asymmetry of the two-channel waveguide and the amplitude of the modes in the lower refractive index waveguide is smaller than that in the higher refractive index waveguide for the self-defocusing medium, while for the self-focusing medium, the amplitude of the modes in the lower refractive index waveguide is larger than that in the higher refractive index waveguide.

We also demonstrate the profiles of optical modes with dependence on the propagation constant β. Figures 4 and 5 present several corresponding modes shown in Figs. 2 and 3 for different propagation constants β. From them, one can see that for self-defocusing media the profile of nonlinear modes shrinks and the corresponding amplitude becomes smaller with an increase of the propagation constant β, while for

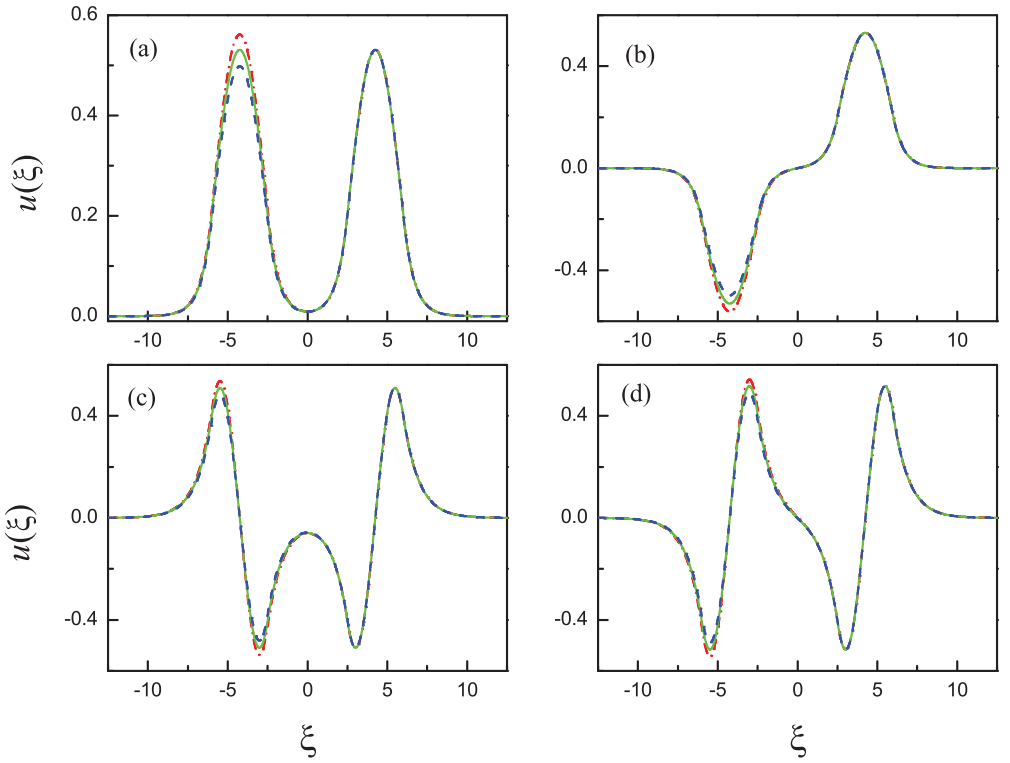

FIG. 3. (Color online) Various different optical modes existing in self-focusing medium ($\eta = 1$), where the dash-dotted red line is the optical mode for $V_1 = 2.500$, the solid green line is the optical mode for $V_1 = 2.525$, and the dashed blue line is the optical mode for $V_1 = 2.550$. Here $\beta = 2.30$ in (a) and (b) and $\beta = 1.10$ in (c) and (d).

self-focusing case it is opposite, namely, the profile of nonlinear modes becomes more prominent and the corresponding amplitude becomes larger. This feature can be depicted by the dispersion relations between the total energy P_0 and the propagation constant β. As shown in Figs. 6 and 7, one can see that the total energy decreases with the increase of

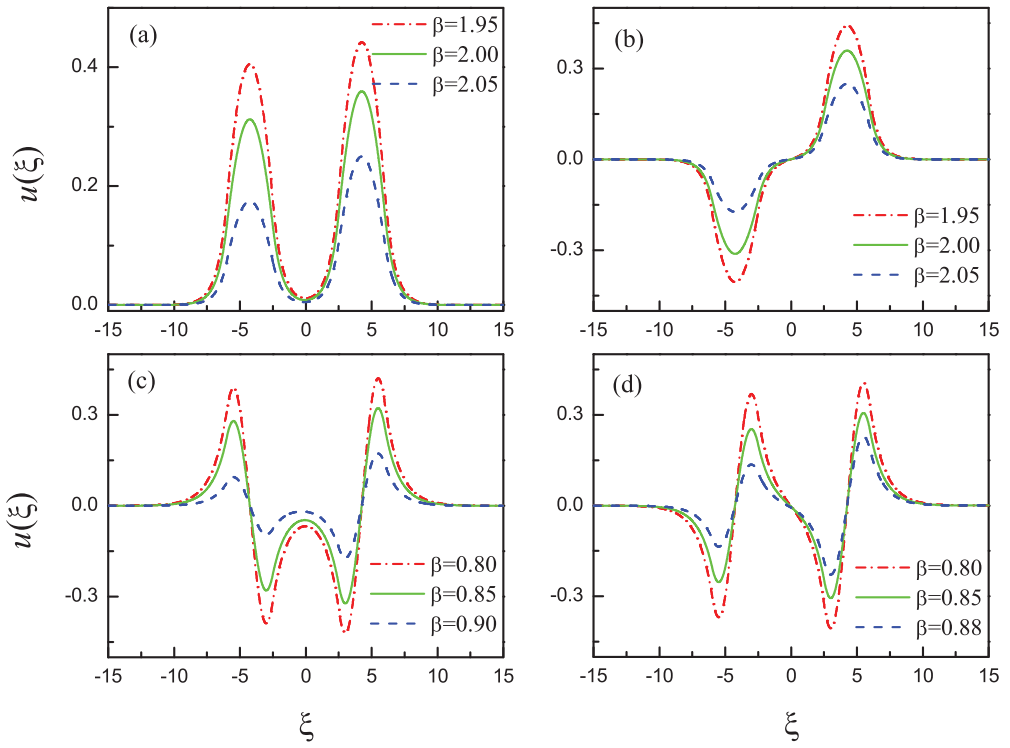

FIG. 4. (Color online) Several optical modes with different β values in a nonlinear asymmetrical double-channel waveguide for the self-defocusing medium ($\eta = -1$). Here the parameters are $V_1 = 2.500$ and $V_2 = 2.525$.

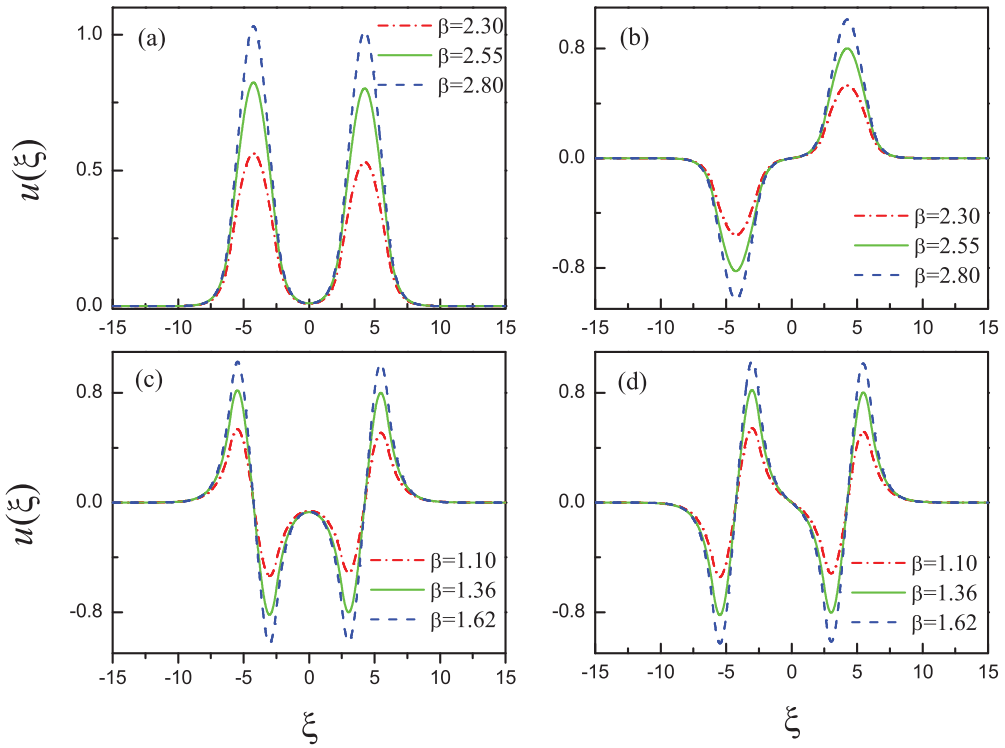

FIG. 5. (Color online) Several optical modes with different β values in a nonlinear asymmetrical double-channel waveguide for the self-focusing medium ($\eta = 1$). Here the parameters are the same as in Fig. 4.

the propagation constant for self-defocusing media (Fig. 6), whereas it is an increasing function of the propagation constant for the self-focusing case (Fig. 7).

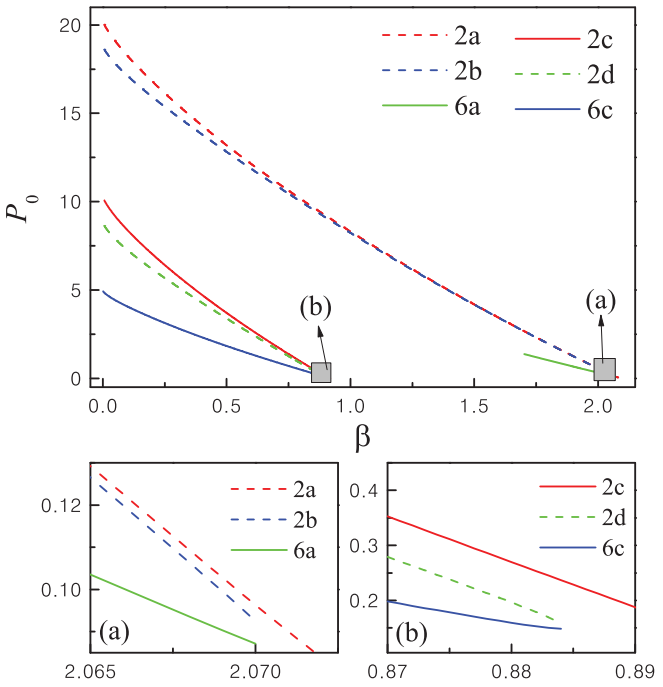

FIG. 6. (Color online) The dependence of the total energy P_0 on the propagation constant β for the modes existing in self-defocusing medium ($\eta = -1$). Here the parameters are $V_1 = 2.500$ and $V_2 = 2.525$. The shaded areas are enlarged in insets (a) and (b). The labels 2a and 2b, and so forth correspond to modes shown in Figs. 2(a) and 2(b), and so forth, respectively.

As discussed in Ref. [36], besides the symmetry-preserving optical modes, a double-channel waveguide also supports the symmetry-breaking optical modes, and the corresponding optical modes in a nonlinear asymmetric double-channel waveguide are presented in Fig. 8, in which we also plotted the corresponding symmetry-breaking optical modes in a symmetric double-channel waveguide for comparison. One finds that the optical modes in a nonlinear asymmetric double-channel waveguide are almost the same as the modes in a symmetric one for the given β.

Similarly, the corresponding modes shown in Fig. 8 for different propagation constants β are presented in Fig. 9. It is shown that the profile of nonlinear modes shrinks with the increase of the propagation constant β for the self-defocusing case, while for the self-focusing case the profile of nonlinear modes becomes more pronounced. This feature is depicted by the dispersion relations between the total energy P_0 and the propagation constant β. It should be pointed out that the modes shown in Fig. 8 exist only in a small region, as shown in Figs. 6 and 7.

From the dispersion relations shown in Figs. 6 and 7, one can see that for the self-defocusing medium there is no intersection between dispersion curves (see Fig. 6 and the enlarged areas), which indicates that no degenerate modes exist, and the total energy of the mode shown in Fig. 2(a) is the highest for a given propagation constant β. While for the self-focusing medium the dispersion curves can intersect [see Figs. 7(c) and 7(d)], which implies that there exist two different modes with the same total energy at the intersection point, namely, that the degeneracy occurs at the intersection point. Note that for our choices of parameters, the intersection points of the dispersion curves for the modes shown in Figs. 3(a)

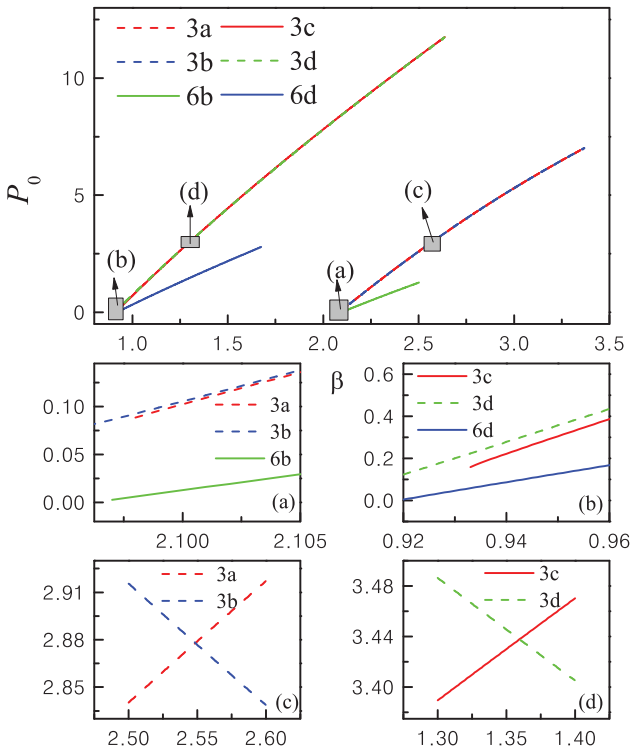

FIG. 7. (Color online) The dependence of the total energy P_0 on the propagation constant β for the modes existing in self-focusing medium ($\eta = 1$). Here the parameters are $V_1 = 2.500$ and $V_2 = 2.525$. The shaded areas are enlarged in (a)–(d). The labels 3a, 3b, and so forth correspond to modes shown in Figs. 3(a) and 3(b), and so forth, respectively.

and 3(b) and in Figs. 3(c) and 3(d) are about 2.5485 and 1.3595, respectively, and the corresponding degenerate modes are shown by the green solid curves in Fig. 5. Here, to distinguish the intersections, we rotate the dispersion curve for the modes shown in Fig. 3(a) [Fig. 3(c)] by an angle of $\pi/6$ counterclockwise, as the center of intersection point and the same angle for dispersion curve of the mode shown in Fig. 3(b) [Fig. 3(d)] are rotated clockwise, as shown in Figs. 7(c) and 7(d).

IV. THE NONLINEAR MANIPULATION OF OPTICAL MODES IN A DOUBLE-CHANNEL WAVEGUIDE

In this section, we demonstrate the control and manipulation of optical modes in reconfigurable nonlinear media. Our interest is to investigate the evolutionary dynamics of optical beams in a double-channel waveguide propagating into a uniform nonlinear medium. In this case, the governing equation can be generally written as

$$i\frac{\partial\psi}{\partial z} + \frac{1}{2k_0}\frac{\partial^2\psi}{\partial x^2} + \frac{k_0\Delta n(z,x)}{n_0}\psi = 0, \tag{12}$$

where the refractive index change $\Delta n(z,x)$ is a function of z and x and $\Delta n(z,x) = n(z,x) - n_0$. Here we assume that when $0 \leqslant z \leqslant Z_0$, $n(z,x)$ is in the form of Eq. (1) and $\Delta n(z,x) = F(x) + n_2 I(z,x) - n_0$; while for $z > Z_0$, $\Delta n(z,x) = n_2' I(z,x) - n_0$. Here, n_2 and n_2' are the Kerr nonlinear coefficients of different media in the regions of $0 \leqslant z \leqslant Z_0$ and $z > Z_0$, respectively. Thus, when $0 \leqslant z \leqslant Z_0$, namely in the region of $0 \leqslant \zeta \leqslant \zeta_0$, Eq. (12) can be

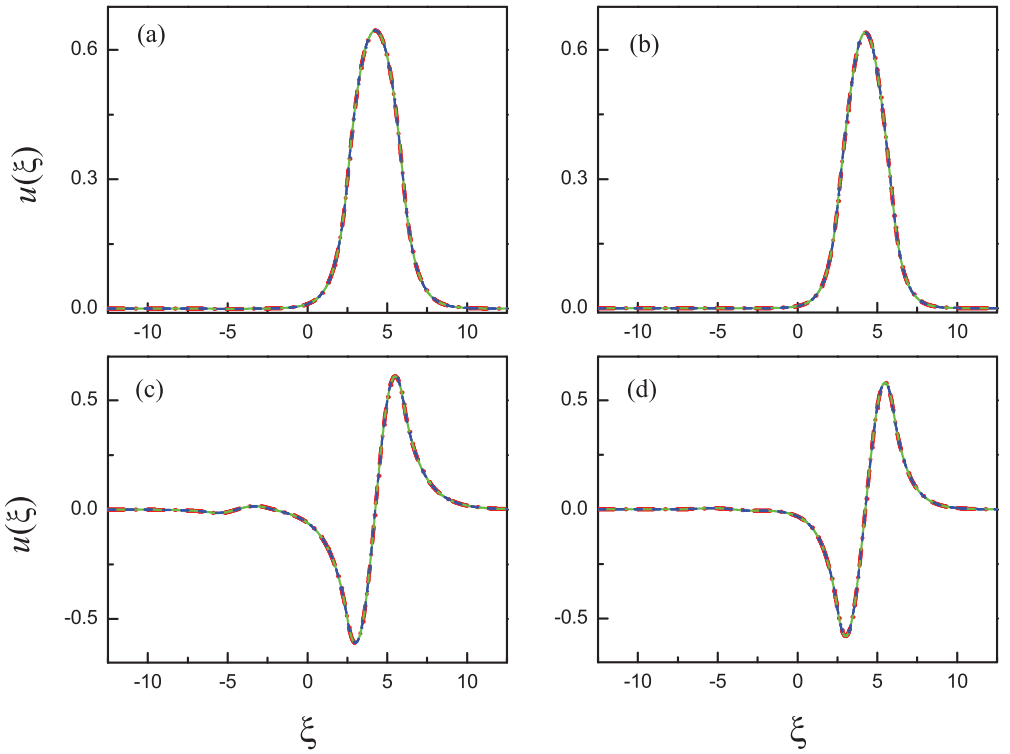

FIG. 8. (Color online) Several symmetry-breaking optical modes, where the dash-dotted red lines are optical modes for $V_1 = 2.500$, the solid green lines are optical modes for $V_1 = 2.525$, and the dashed blue lines are optical modes for $V_1 = 2.550$. Here $\eta = -1$ in (a) and (c), $\eta = 1$ in (b) and (d), $\beta = 1.78$ in (a), $\beta = 2.39$ in (b), $\beta = 0.66$ in (c), and $\beta = 1.15$ in (d).

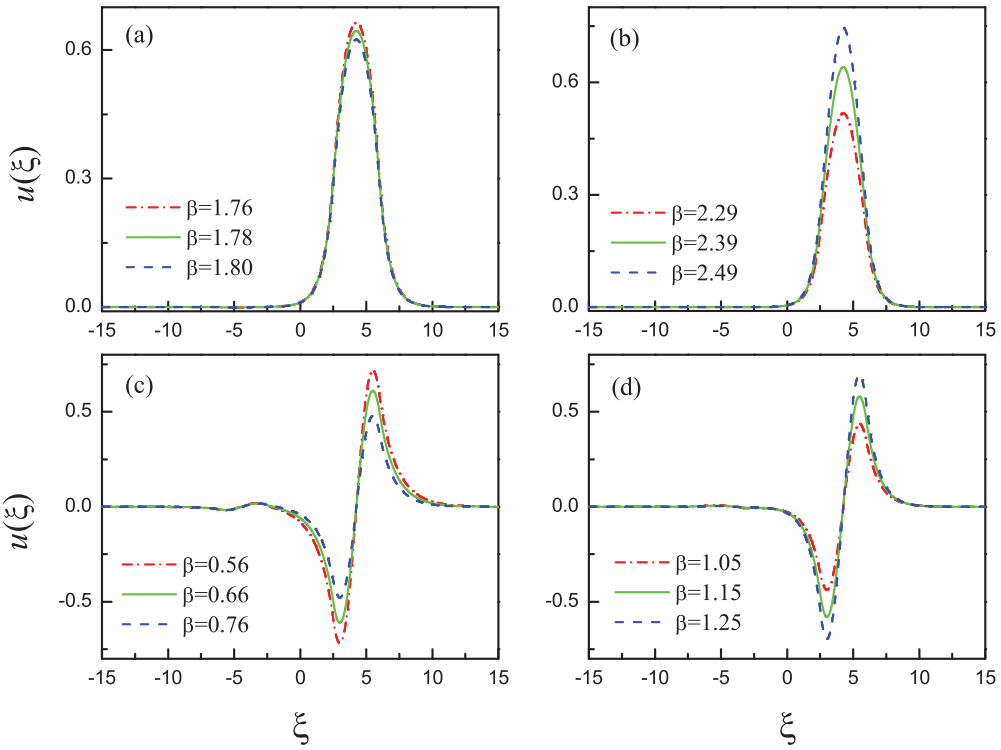

FIG. 9. (Color online) Several symmetry-breaking optical modes with different β values in a nonlinear asymmetrical double-channel waveguide. Here the parameters are the same as in Fig. 8.

normalized to Eq. (3), where $\zeta = z/L_D$ and $\zeta_0 = Z_0/L_D$ with $L_D = 2k_0 w_0^2$. At the same time, in the region of $z > Z_0$, namely $\zeta > \zeta_0$, Eq. (12) is reduced to the dimensionless form as follows:

$$i\frac{\partial \varphi}{\partial \zeta} + \frac{\partial^2 \varphi}{\partial \xi^2} + \eta' |\varphi|^2 \varphi = 0, \tag{13}$$

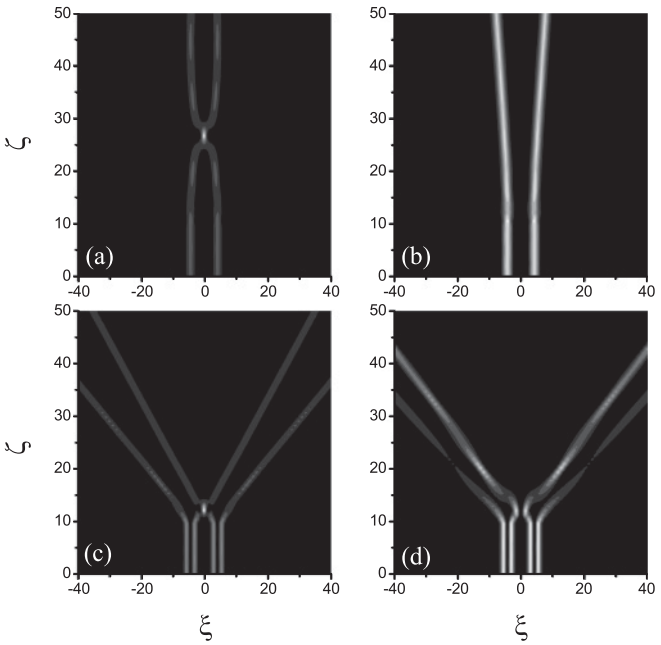

FIG. 10. The evolution of optical modes shown in Fig. 2 into the self-focusing Kerr medium without channels, where $\eta' = 10$ in (a) and (b) and $\eta' = 20$ in (c) and (d). Here the parameters are $V_1 = V_2 = 2.525$ and $\zeta_0 = 10$. The labels (a)–(d) correspond to modes shown in Figs. 2(a)–2(d), respectively.

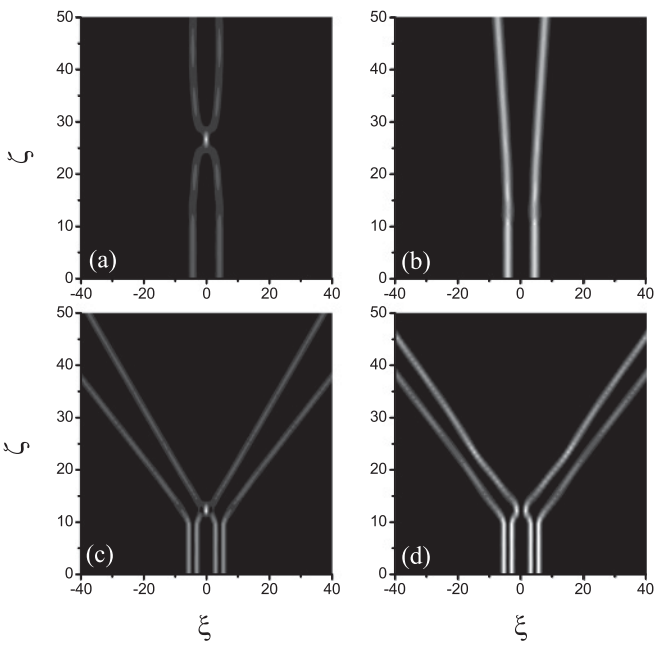

FIG. 11. The evolution of optical modes shown in Fig. 3 into the self-focusing Kerr medium without channels, where $\eta' = 5$ in (a) and (b) and $\eta' = 10$ in (c) and (d). Here the parameters are $V_1 = V_2 = 2.525$ and $\zeta_0 = 10$. The labels (a)–(d) correspond to modes shown in Figs. 3(a)–3(d), respectively.

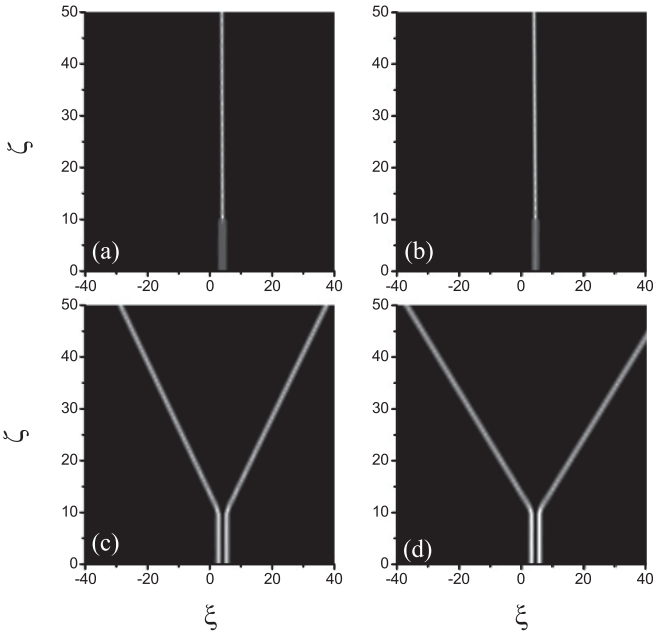

FIG. 12. The evolution of optical modes shown in Fig. 8 into the self-focusing Kerr medium without channels, where $\eta' = 10$. Here the parameters are $V_1 = V_2 = 2.525$ and $\zeta_0 = 10$. The labels (a)–(d) correspond to modes shown in Figs. 8(a)–8(d), respectively.

where $\eta' = n_2'/|n_2|$. Note that Eq. (13) is different from Eq. (3), in which Eq. (3) includes a potential function $V(\xi)$ given by Eq. (4), while Eq. (13) does not include and can describe the dynamics of beams in Kerr media without any refractive index modulation.

In the following analysis, optical beams of different modes existing in double-channel waveguides are injected into the uniform nonlinear medium after propagating diffraction length of ζ_0 in double-channel waveguide.

First, we consider the situation that optical beams are injected from symmetrical double-channel waveguide. For the optical modes shown in Fig. 2, which exist in a self-defocusing medium ($\eta = -1$), the numerical simulations show that when $\eta' < 0$, these optical modes are diffracted quickly after entering a uniform Kerr medium. However, when $\eta' > 0$ and is large enough, the evolution of optical beams exhibits different scenarios in the Kerr medium without any channels, as shown in Fig. 10. Similarly, for the optical modes shown in Fig. 3, which exist in self-focusing media ($\eta = 1$) with double-channel waveguide, as shown in Fig. 11, our numerical simulations show that the evolution of optical modes exhibit properties similar to those in Fig. 10.

From Figs. 10 and 11, one can see that when the optical modes existing both in self-defocusing and self-focusing media with a double-channel waveguide are injected into the self-defocusing medium without any channels, the beams should be diffracted quickly. However, when the optical

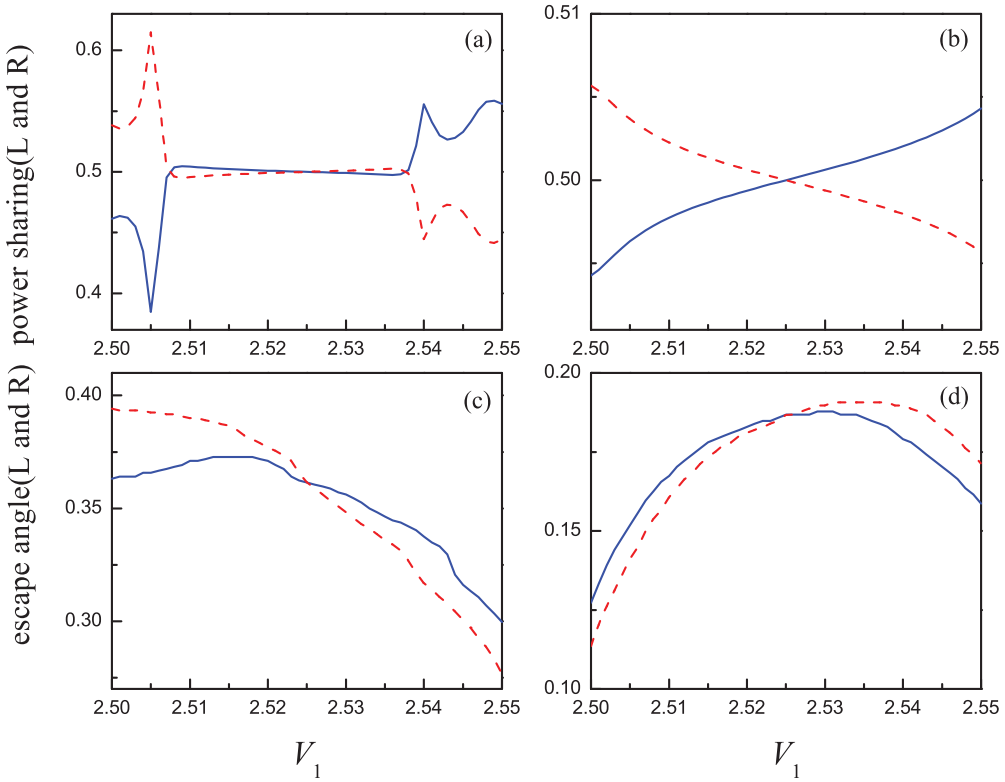

FIG. 13. (Color online) Energy sharing (row 1) and escape angles (row 2) of optical beams as a function of parameter V_1. In all cases, the solid-blue and the dashed-red curves correspond to the left and right beams, respectively. Here the parameters are $V_2 = 2.525$, $\eta' = 10$ in (a) and (c), which correspond to the modes shown in Fig. 2(b) [namely Fig. 11(b)], and $\eta' = 5$ in (b) and (d), which correspond to the modes shown in Fig. 3(b) [namely Fig. 12(b)].

modes are injected into the self-focusing medium without any channels and the corresponding nonlinear coefficient η' is larger, the beams could be manipulated effectively. In this situation, when the optical modes shown in Figs. 2(a) and 3(a) are injected into self-focusing medium without any channels, the beams appear to attract and repel each other periodically, as shown in Figs. 10(a) and 11(a). When the modes shown in Figs. 2(b)–2(d) and Figs. 3(b)–3(d) are injected into self-focusing medium without any channels, the beams repel each other, as shown in Figs. 10(b)–10(d) and Figs. 11(b)–11(d). Note that the escape angles are the same for the beams in Fig. 2(b) [Fig. 3(b)] due to the symmetry of the double-channel waveguide.

The evolution of optical modes shown in Fig. 8 is presented in Fig. 12, in which Figs. 12(a) and 12(c) [Figs. 12(b) and 12(d)] demonstrate the evolution of optical modes in the self-focusing medium without any channels with initial input beams injected from self-defocusing (self-focusing) medium with double-channel waveguide. As shown in Figs. 12(a) and 12(b), one can see that optical beams with a single hump can be compressed effectively. and as shown in Figs. 12(c) and 12(d) the optical modes with two peaks are separated during the evolution due to the repulsive interaction force resulting from the phase difference between the two peaks.

It should be pointed out that these results take into account only the optical modes existing in the symmetrical double-channel waveguide. Then, we are curious about the influence of the asymmetrical double-channel on the evolution of optical modes. In order to understand this question, we launch optical beams from an asymmetrical double-channel waveguide into the self-focusing medium to observe their evolution by tuning the depth of left channel of the waveguide for a fixed depth of the right channel; namely, the value of V_1 varies from 2.500 to 2.550 for $V_2 = 2.525$. As an example, we demonstrated the evolution dynamics for the modes shown in Figs. 2(b) and 3(b). In Fig. 13, we present the dependence of the energy sharing (the ratio of the energy carried by each component in the mode over the total energy) and the escape angle (the angle of the each peak in the mode and the propagation direction ζ) on the value of V_1. As shown in Fig. 13, one can see that the energy carried by each beam is different due to the asymmetry of the double-channel waveguide [shown in Figs. 13(a) and 13(b)]. Also, one can see clearly that the escape angles of the two beams take different values with the change of the value V_1, which means that the beams can be controlled by tuning the depth of the left channel of the waveguide.

V. CONCLUSION

We have studied light-beam propagation in an asymmetric double-channel waveguide in the form of a nonlinear coupler. A family of analytical solutions with symmetric and antisymmetric forms has been obtained for both self-focusing and self-defocusing nonlinear media, and the dispersion relations between the total energy and the propagation constant has been discussed in detail. Our results reveal that the system with self-focusing nonlinear response supports the degenerate modes, while for self-defocusing medium the degenerate modes do not exist. In addition, we explored new ways to steer optical modes propagating from double-channel waveguide into a uniform self-focusing medium. The compression of beam with single hump and split of beams with two humps have been demonstrated by tuning the depth of the channel of the waveguide. These properties may be applied in practical optical devices and may be useful for optical processing, optical switching, or optical routing.

ACKNOWLEDGMENT

The authors acknowledge fruitful discussions with Professor Yuri Kivshar. This research is supported by the National Natural Science Foundation of China Grant No. 61078079, the Shanxi Scholarship Council of China Grant No. 2011-010, and the Australian Research Council.

[1] S. Longhi, Laser Photon. Rev. **3**, 243 (2009).
[2] W. J. Tomlinson, Opt. Lett. **5**, 323 (1980).
[3] V. K. Fedyanin and D. Mihalache, Z. Phys. B **47**, 167 (1982); D. Mihalache, R. G. Nazmitdinov, and V. K. Fedyanin, Physica Scripta **29**, 269 (1984); D. Mihalache, D. Mazilu, and H. Totia, *ibid.* **30**, 335 (1984).
[4] N. N. Akhmediev, Zh. Eksp. Teor. Fiz. **83**, 545 (1982) [Sov. Phys. JETP **56**, 299 (1982)].
[5] G. I. Stegeman, C. T. Seaton, J. Chilwell, and S. D. Smith, Appl. Phys. Lett. **44**, 830 (1984).
[6] N. N. Akhmediev, V. I. Korneyev, and Y. V. Kuzmenko, Zh. Eksp. Teor. Fiz. **88**, 107 (1985).
[7] F. Lederer and D. Mihalache, Solid State Commun. **59**, 151 (1986); D. Mihalache, D. Mazilu, and F. Lederer, Opt. Commun. **59**, 391 (1986).
[8] D. Mihalache, G. I. Stegeman, C. T. Seaton, E. M. Wright, R. Zanoni, A. D. Boardman, and T. Twardowski, Opt. Lett. **12**, 187 (1987).
[9] D. Mihalache, M. Bertolotti, and C. Sibilia, Prog. Opt. **27**, 229 (1989).
[10] U. Langbein, F. Lederer, T. Peschel, U. Trutschel, and D. Mihalache, Phys. Rep. **194**, 325 (1990).
[11] A. D. Boardman, P. Egan, U. Langbein, F. Lederer, and D. Mihalache, in *Nonlinear Surface Electromagnetic Phenomena*, edited by H. E. Ponath and G. I. Stegeman (North-Holland, Amsterdam, 1991), pp. 73–287.
[12] F. Lederer, L. Leine, R. Muschall, T. Peschel, C. Schmidt-Hattenberger, T. Trutschel, A. D. Boardman, and C. Wachter, Opt. Commun. **99**, 95 (1993).
[13] A. R. Davoyan, I. V. Shadrivov, and Y. S. Kivshar, Opt. Express **16**, 21209 (2008).
[14] D. Marcuse, J. Lightwave Technol. **5**, 113 (1987).
[15] C. C. Yang, Opt. Lett. **16**, 1641 (1991).
[16] C. C. Yang and A. J. S. Wang, IEEE J. Quantum Electron. **28**, 479 (1992).
[17] Y. Chen, Opt. Quantum Electron. **24**, 539 (1992).

[18] K. Yasumoto, H. Maeda, and N. Maekawa, J. Lightwave Technol. **14**, 628 (1996).
[19] D. N. Christodoulides, F. Lederer, and Y. Silberberg, Nature (London) **424**, 817 (2003).
[20] F. Lederer, G. I. Stegeman, D. N. Christodoulides, G. Assanto, M. Segev, and Y. Silberberg, Phys. Rep. **463**, 1 (2008).
[21] Y. V. Kartashov, V. A. Vysloukh, and L. Torner, Prog. Opt. **52**, 63 (2009).
[22] H. S. Eisenberg, Y. Silberberg, R. Morandotti, A. R. Boyd, and J. S. Aitchison, Phys. Rev. Lett. **81**, 3383 (1998); D. Mandelik, H. S. Eisenberg, Y. Silberberg, R. Morandotti, and J. S. Aitchison, *ibid*. **90**, 053902 (2003).
[23] M. J. Ablowitz and Z. H. Musslimani, Phys. Rev. Lett. **87**, 254102 (2001).
[24] Y. Lahini, E. Frumker, Y. Silberberg, S. Droulias, K. Hizanidis, R. Morandotti, and D. N. Christodoulides, Phys. Rev. Lett. **98**, 023901 (2007).
[25] J. W. Fleischer, M. Segev, N. K. Efremidis, and D. N. Christodoulides, Nature (London) **422**, 147 (2003); J. W. Fleischer, T. Carmon, M. Segev, N. K. Efremidis, and D. N. Christodoulides, Phys. Rev. Lett. **90**, 023902 (2003).
[26] D. Neshev, E. Ostrovskaya, Y. Kivshar, and W. Krolikowski, Opt. Lett. **28**, 710 (2003).
[27] Y. V. Kartashov, V. A. Vysloukh, and L. Torner, Phys. Rev. Lett. **93**, 153903 (2004).
[28] Y. P. Zhang and B. Wu, Phys. Rev. Lett. **102**, 093905 (2009).
[29] J. Proctor and J. Kutz, Opt. Lett. **30**, 2013 (2005).
[30] A. B. Aceves, C. De Angelis, T. Peschel, R. Muschall, F. Lederer, S. Trillo, and S. Wabnitz, Phys. Rev. E **53**, 1172 (1996).
[31] H. F. Zhang, J. Jia, S. T. Jia, and L. Li, Opt. Commun. **281**, 4130 (2008).
[32] Z. Xu, M. I. Molina, and Y. S. Kivshar, Phys. Rev. A **80**, 013817 (2009).
[33] Y. V. Kartashov, B. A. Malomed, and L. Torner, Rev. Mod. Phys. **83**, 247 (2011).
[34] P. G. Kevrekidis, Z. Chen, B. A. Malomed, D. J. Frantzeskakis, and M. I. Weinstein, Phys. Lett. A **340**, 275 (2005).
[35] Z. Birnbaum and B. A. Malomed, Phys. D **237**, 3252 (2008).
[36] J. F. Jia, Y. P. Zhang, W. D. Li, and L. Li, Opt. Commun. **283**, 132 (2010).
[37] T. Pertsch, P. Dannberg, W. Elflein, A. Brauer, and F. Lederer, Phys. Rev. Lett. **83**, 4752 (1999).
[38] W. D. Li, Phys. Rev. A **74**, 063612 (2006).
[39] P. F. Byrd and M. D. Friedman, *Handbook of Elliptic Integrals for Engineers and Scientists*, 2nd ed. (Springer-Verlag, New York, 1971).